Submitted to Zeitschrift fuer Physik

LBL-5812
Preprint c.1

EVIDENCE FOR THE CHARACTERIZATION OF HEAVY-ION REACTIONS BY THE RATIO E/B

G. J. Mathews, G. J. Wozniak, R. P. Schmitt, and
L. G. Moretto

November 1976

Prepared for the U. S. Energy Research and
Development Administration under Contract W-7405-ENG-48

EVIDENCE FOR THE CHARACTERIZATION OF HEAVY-ION REACTIONS BY THE RATIO E/B*

G. J. Mathews†, G. J. Wozniak, R. P. Schmitt, and L. G. Moretto
Nuclear Science Division
Lawrence Berkeley Laboratory
University of California
Berkeley, California 94720

ABSTRACT

The connection between the characteristic features of reactions involving very heavy target-projectile combinations (e.g. $^{86}Kr + {}^{197}Au$) and lighter systems (e.g. $^{40}Ar + {}^{nat}Ag$) is discussed. Evidence for an empirical scaling law based upon the ratio E/B (center-of-mass kinetic energy to Coulomb barrier) is presented. This scaling is justified in terms of semi-quantitative arguments whereby the different charge and angular distribution patterns from light and heavy target-projectile combinations are correlated with different lifetime regimes for the "intermediate complex" as it diffuses along the mass-asymmetry coordinate.

*This work was done with support from the U.S. Energy Research and Development Administration.

†AWU-ERDA Fellow on leave from the University of Maryland.

INTRODUCTION

Two very different patterns have been observed in heavy-ion collisions. On the one hand, features of the "quasi-fission" process [1] are characterized by rather narrow mass (or charge) distributions and side-peaked gross-product (all masses) angular distributions. This phenomenon has been observed in relatively heavy projectile-target collisions. [1-3] On the other hand, the label "deep-inelastic scattering" has generally been applied to lighter projectile-target systems [4-8] where the observed features are: relatively broad mass distributions, and forward-peaked angular distributions.

Detailed studies [9] of the reaction ^{197}Au + 620 MeV ^{86}Kr provided strong evidence that the two patterns of angular distributions are not necessarily due to different mechanisms, but can be associated with differences in the lifetime of the "intermediate complex." The angular distributions for this reaction show a continuous transition from side peaking to forward peaking which can be explained by the effective increase in the lifetime of the complex due to the delay in populating asymmetries far removed from that of the entrance channel. In light of the above observations, it certainly seems plausible that the lifetime of the intermediate complex is the key to understanding the different patterns observed in light and heavy systems. The success of diffusion model calculations [9], which incorporated an ℓ-dependent lifetime, suggests that the lifetime of the intermediate complex is dynamically controlled. A recent survey [10] of the existing data seems to show a correlation between the ratio E/B and the system's average lifetime. To test this hypothesis, we have attempted to introduce side peaking in a light system by decreasing the bombarding energy.

In this paper we compare recent data obtained at LBL's 88-inch cyclotron from a study of the bombardment of a natural silver target $^{nat}Ag(52\%\ ^{107}Ag,\ 48\%\ ^{109}Ag)$ with a 170 MeV ^{40}Ar beam with previously published data on the same system at a higher bombarding energy [11] and with two examples obtained from Kr reaction studies [9,12]. (All these data were obtained with a ΔE-E telescope which allows the identification of individual atomic numbers up to $Z \sim 50$.) These data provide evidence for the characterization of a system's charge and angular distributions by the ratio E/B. A semi-quantitative model will be described which attempts to justify the observed E/B scaling by relating this ratio to the product of the lifetime and rotational velocity (i.e. the rotation angle) of the intermediate complex.

RESULTS

Charge and mass distributions obtained in a wide variety of target-projectile combinations have been interpreted by Moretto and Sventek [13] in terms of a diffusion model employing the Master equation and by Nörenberg [14] using the Fokker-Planck equation. For the sake of simplicity, we shall take the latter approach. In a diffusion model the characteristic features of the mass (or charge) distribution are intimately related to the lifetime of the system. For example, a solution to the Fokker-Planck equation for a mass-asymmetry driving potential of constant slope is:

$$\phi(Z,t) = \frac{1}{\sqrt{2\pi\mu_2 t}} \exp\left[-\frac{[(Z-Z_0) - \mu_1 t]^2}{2\mu_2 t}\right], \qquad (1)$$

where $\phi(Z,t)$ is the population of element Z at time t, and Z_o is the injection point. The quantities μ_1 and μ_2 are velocities given by,

$$\mu_1 = \int_{Z-1}^{Z+1} (Z'-Z)\ \Lambda_{Z'Z}\ dZ' \quad ,$$

$$\mu_2 = \int_{Z-1}^{Z+1} (Z'-Z)^2\ \Lambda_{Z'Z}\ dZ' \quad , \tag{2}$$

where $\Lambda_{Z'Z}$ is a macroscopic transition probability [13]. The charge (or mass) distribution described by Eq. (1) is that of a Gaussian which drifts and broadens in time. The variance σ^2 of the charge distribution is given by

$$\sigma^2 = \mu_2 t \quad , \tag{3}$$

so that narrow and broad charge distributions correspond to short and long lifetimes, respectively.

Angle-integrated charge distributions for four reactions are presented in order of increasing values of E/B in Figs. 1 and 2. For the first three reactions the observed angular range extended both before and behind the grazing angle while the 340 MeV $^{40}Ar + {}^{nat}Ag$ data do not extend forward of the grazing angle. To facilitate comparison, the members of each pair of distributions in both Figs. 1 and 2 have been shifted to align the entrance channels (the projectile Z-value has been left off both figures because of serious background contamination).

Comparing the four spectra in Figs. 1 and 2, it is evident that the width of the charge distributions increases dramatically as the ratio E/B increases. For an E/B of 1.2 (170 MeV ^{40}Ar + ^{nat}Ag) the peak in the integrated charge distribution centered at the projectile is very narrow (see Fig. 1a). (The second peak at symmetry could be due to compound nucleus fission [15] or enhanced diffusion toward symmetry and does not affect the conclusions of this work). When E/B is increased to 1.4 (620 MeV ^{86}Kr + ^{197}Au), the integrated charge distribution broadens dramatically although it is still centered at the projectile Z-value (see Fig. 1b). If E/B is raised to 1.8 (620 MeV ^{86}Kr + ^{nat}Ag), the integrated charge distribution is broader still and a drift toward symmetry is observed in the centroid (see Fig. 2a). For a still larger value of E/B = 2.3 (340 MeV ^{40}Ar + ^{nat}Ag), the integrated charge distribution becomes relatively flat with no evidence of any peaking near the projectile Z-value (see Fig. 2b). Insofar as these Z-distributions can be interpreted in terms of a diffusion process, the increasing charge widths imply longer lifetimes for the systems which are correlated with increasing values of E/B. (One should note that we are referring to an average lifetime since there may well be a distribution of lifetimes associated with the different ℓ-waves, for example).

In Figs. 3 and 4 angular distributions are shown for the detected products from the above four reactions. One is immediately struck by the very different patterns present in the distributions* for the systems

*Note that the cross section for the 620 MeV ^{86}Kr + ^{nat}Ag system is plotted as $d\sigma/d\theta$ and that forward peaking is manifested by a straight line with negative slope.

with values of E/B $\lesssim 1.5$ compared to those with values of E/B > 1.5 . For the two reactions with low values of E/B, extensive side peaking occurs in the angular distributions of elements near the projectile Z; whereas, for the two reactions with larger values of E/B, no side peaking is observed other than that due to quasi-elastic events, which appear as a distinct component in the energy spectra for the 620 MeV Kr + ^{nat}Ag system.

The above trends in the angular distribution patterns are consistent with the formation of an intermediate complex whose lifetime depends on the value of E/B. If the ratio of the lifetime of the intermediate complex to its rotational period is small, then fragments produced in the diffusion process will be emitted on the side of impact. For larger values of this ratio, the complex may rotate to angles near 0° before decaying, producing a forward peaked (in excess of $1/\sin\theta$) angular distribution. In the event that the lifetime is long relative to the rotational period, a $1/\sin\theta$ angular distribution will be produced.

One observes side peaking near the projectile Z-value (see Fig. 3a) in the system 170 MeV ^{40}Ar + ^{nat}Ag (E/B = 1.2), which indicates that the lifetime of the intermediate complex is small relative to its rotational period. However, for large mass transfers $1/\sin\theta$ angular distributions occur. For the case of 620 MeV ^{86}Kr + ^{197}Au (E/B = 1.4) side peaking is also observed (see Fig. 3b). One should note that in both of the above systems there is no clear-cut distinction between quasi-elastic and deep-inelastic processes; only a single broad peak is seen near the grazing angle.

For the case of 620 MeV ^{86}Kr + ^{nat}Ag, the angular distributions are for the most part forward peaked (see Fig. 4a). Although there is some weak side peaking for a few elements on either side of the projectile, it is entirely due to the separable quasi-elastic component (see Fig. 4a). The extensive forward peaking indicates that the average system lifetime is long enough so that rotation can proceed through 0° (i.e. orbiting). In Fig. 4b are shown the angular distributions for two systems with longer lifetimes, 288 MeV (E/B = 2.0) and 340 MeV (E/B = 2.3) ^{40}Ar + ^{nat}Ag, which are strongly forward peaked. A comparison of these data with those in Fig. 3a demonstrates that it is possible to change the angular distribution pattern from a forward- to a side-peaked one by simply decreasing the bombarding energy. A more complete set of data for a large variety of target-projectile combinations is summarized in Table 1. These data indicate that side-peaked angular distributions (short lifetimes) tend to occur for values of E/B $\lesssim$ 1.5 and forward-peaked distributions for larger values of E/B; providing further evidence for the characterization of heavy-ion reactions by this parameter.

DISCUSSION

To justify the apparent connection between the ratio E/B and the observed characteristics of the charge and angular distributions, in the former case, one must relate this factor to the system lifetime and, in the latter, to the ratio of the lifetime to the rotational period (or, equivalently, the rotation angle). To do this let us consider a very simple picture, namely that of an "idealized" system which contains only a Coulomb interaction and no dissipative forces. We shall see that for this system the E/B scaling law follows.

Consider the quantity:

$$\frac{E}{B} - 1 = \frac{E - B}{B} . \qquad (4)$$

Provided that the Coulomb barrier is close to the interaction barrier, the above quantity can be written as follows:

$$\frac{E - B}{B} \simeq \frac{\mu v_o^2 R}{2Z_1 Z_2} = \frac{1}{4}\left[\frac{2\mu v_o R^2}{Z_1 Z_2}\right]\left[\frac{v_o}{R}\right] = \frac{1}{2}\left[2\mu \frac{v_o}{\sqrt{2}} \frac{R^2}{Z_1 Z_2}\right]\left[\frac{v_o}{\sqrt{2}} \frac{1}{R}\right] \qquad (5)$$

where μ is the reduced mass of the target-projectile at the interaction radius R; v_o is the center-of-mass velocity at the same radius; and Z_1, Z_2 are the target and projectile charges.

Let us now consider an impact parameter such that the radial and tangential velocities are equal (i.e. ℓ_{rms}). At the interaction radius these velocities are $\frac{v_o}{\sqrt{2}}$. Then the first square bracket in the last expression represents the time it takes the system, subject to a force equal to the Coulomb force at the interaction radius, to move in and out along its radial coordinate. For a moderate value of v_o the first square bracket can be identified with the system lifetime:

$$\tau_{life} = 2\,\frac{\mu v}{c} \simeq 2\,\frac{v_o}{\sqrt{2}}\,\mu\,\frac{R^2}{Z_1 Z_2} = \frac{\sqrt{2}\,\hbar\,\ell_{max}}{B} \;, \tag{6}$$

where v is the velocity; c is the force; ℓ_{max} is the maximum ℓ wave associated with the reaction. Thus we see that this simple model predicts that the lifetime increases as the ratio E/B increases which in the case of a diffusive mechanism predicts a broader charge distribution for a larger E/B.

The second square bracket in eq. (5) is just the angular velocity (assuming no sticking and no dissipation). The product of the two brackets is the angle of rotation of the complex, prior to decay:

$$\theta_{Rot} = 2\left(\frac{E}{B} - 1\right). \tag{7}$$

If the rotation of 1 radian is a good criterion for discriminating between orbiting past 0° and side decay, we then obtain:

$$1 = 2\left(\frac{E}{B} - 1\right), \quad \text{or} \quad \left(\frac{E}{B} \simeq 1.5\right), \tag{8}$$

and one would expect side-peaked angular distributions for E/B $\lesssim$ 1.5 and forward-peaked ones for larger values. Of course, one should add an angular term to Eq. (7) which takes the deflection arising from the Coulomb field into account. However, this term is a monotonically increasing function of E/B and will not effect the overall validity of the scaling.

The success of this idealized model in predicting the observed dependence of the charge widths and angular distributions is encouraging, however, a more realistic approach must take viscosity into account. To estimate the possible effect of a viscous force on Eq. (5), we have integrated the equations of motion for a system with a potential of constant slope and a frictional force proportional to the velocity, and have assumed that the radial and angular equations are uncoupled. We find in this case that both the lifetime and angular velocity can decrease by as much as 30% for a large viscosity coefficient. This reduction introduces an additional factor on the right-hand side of Eq. 5. However, one expects that in a complete solution to the equations of motion which properly account for the nuclear potential there will be some cancelation of the effect of viscous forces. This cancelation would arise from the increase in the lifetime of the system caused by the deepening of the effective potential due to the transformation of orbital angular momentum into intrinsic angular momentum. However, the fact that the simple model considered above predicts the experimentally observed trend implies that there is some sort of cancelation of such effects. To properly account for the above dynamical effects, an effort is being made to incorporate them into diffusion model calculations.

In Table I the lifetime of the intermediate complex for ℓ_{rms} has been estimated using Eq. (6). For the system 620 MeV $^{86}Kr + {}^{197}Au$ one obtains good agreement between the estimate (8.3×10^{-22} sec) from Eq. (6) and the corresponding value (11.7×10^{-22} sec) obtained from diffusion model calculations [9]. One can also obtain estimates of the

the centroids and variances of the charge distributions using this simple model. From Eq. (1) we see that the centroids and variances should scale with the system lifetime provided that the potential energy as a function of mass asymmetry does not deviate significantly from a constant slope over the range of diffusion. Although the latter is a crude approximation, it is of some interest to test this assumption by predicting the widths of the charge distributions with Eq. (3). Expanding Eq. (2) for μ_2 according to the procedure described elsewhere [10] and assuming that $\frac{\partial V}{\partial Z}\frac{1}{T}$ is small and independent of ℓ (a rather crude approximation), one can write an approximate expression for μ_2 :

$$\mu_2 = \frac{4}{3}\pi\kappa\frac{R_1R_2}{R_1+R_2}d, \tag{9}$$

where κ is taken [10] to be $0.5\times10^{21}\ \frac{\text{charge units}}{\text{sec.fm}^2}$, and $d = 1.0$ fm corresponds to the distance over which diffusion occurs. If the values of τ_{life} and μ_2 estimated from Eqs. (6) and (9) represent approximate averages, then the calculated variances ($\mu_2\tau_{life}$) given in Table 1 may roughly correspond to the variances of the experimental total charge distributions. For 170 MeV ^{40}Ar + ^{nat}Ag, for example, we estimate a variance of 3.0 compared to the experimental value of 1.7 obtained by a Gaussian fit to the charge distribution in Fig. 1a (omitting points in the interval $16 < Z < 20$ and after subtracting out the symmetric component). At higher energies where the lifetime of the intermediate complex is longer and the potential deviates significantly from a constant slope we expect to underestimate the distribution widths. In particular, for these long times the ℓ-dependent drift (due to changes in $\partial V/\partial Z$ for different ℓ-waves) will generate an envelope of Gaussians with the centroids distributed over a large range, thus making the experimental widths far larger than our estimates (i.e. we estimate a variance of ~ 7, compared to an experimental value of ~ 76 obtained from a Gaussian fit to the Kr + Ag charge distribution, see Fig. 2a). Nevertheless, the overall trend in the data towards broadening at higher energies is reproduced by the calculations (see Table 1).

CONCLUSIONS

The apparent dichotomy presented by reaction studies of light and heavy systems can be explained by differences in the average lifetime of the system. This conclusion is supported by the fact that it is possible to induce "quasi-fission" behavior in a relatively light system, $^{40}Ar + {}^{nat}Ag$ at a low bombarding energy (170 MeV). A comparison of the charge and angular distributions from several reactions reveal a strong dependence of the charge and angular distribution patterns on the ratio E/B. Within the framework of an "idealized" model it is possible to relate this quantity with the product of the lifetime and rotational velocity of the intermediate complex.

REFERENCES

1) F. Hanappe, M. Lefort, C. Ngô, J. Péter, and B. Tamain, Phys. Rev. Lett. 32, 738 (1974).

2) K. L. Wolf, J. P. Unik, J. R. Huizenga, J. Birkelund, H. Freiesleben, and V. E. Viola, Phys. Rev. Lett. 33, 1105 (1974).

3) R. Vandenbosch, M. P. Webb, and T. D. Thomas, Phys. Rev. Lett. 36, 459 (1976).

4) A. G. Artukh, G. F. Gridnev, V. L. Mikheev, V. V. Volkov, and J. Wilczynski, Nucl. Phys. A215, 91 (1973).

5) B. Gatty, D. Guerreau, M. Lefort, X. Tarrago, J. Galin, B. Cauvin, J. Girard, and H. Nifenecker, Nucl. Phys. A253, 511 (1975).

6) L. G. Moretto, J. Galin, R. Babinet, Z. Fraenkel, R. Schmitt, R. Jared, and S. G. Thompson, Nucl. Phys. A259, 172 (1976).

7) J. C. Jacmart, P. Colombani, H. Doubre, N. Frascaria, N. Poffé, M. Riou, J. C. Roynette, C. Stéphan, and A. Weidinger, Nucl. Phys. A242, 175 (1975).

8) J. B. Natowitz, M. N. Namboodiri, and E. T. Chulick, Phys. Rev. C13, 171 (1976).

9) L. G. Moretto, B. Cauvin, P. Glässel, R. Jared, P. Russo, J. Sventek, and G. Wozniak, Phys. Rev. Lett. 36, 1069 (1976). P. Russo, R. P. Schmitt, G. J. Wozniak, R. C. Jared, P. Glässel, B. Cauvin, J. S. Sventek, and L. G. Moretto, to be published in Nuclear Physics.

10) L. G. Moretto and R. P. Schmitt, European Conference on Nuclear Physics with Heavy Ions, Caen, 1976 (LBL-5057).

11) J. Galin, L. G. Moretto, R. Babinet, R. Schmitt, R. Jared, and S. G. Thompson, Nucl. Phys. A255, 472 (1975).

12) R. P. Schmitt, P. Russo, R. Babinet, R. Jared, and L. G. Moretto, LBL-5042, Nuclear Physics (in press).

13) L. G. Moretto and J. S. Sventek, Phys. Lett. 58B, 26 (1975), and Proceedings of the Symposium on Macroscopic Features of Heavy Ion Collisions, Argonne, 1976 (LBL-5006).

14) W. Nörenberg, Phys. Lett. 53B, 289 (1974).

15) H. C. Britt, B. H. Erkkila, R. H. Stokes, H. H. Gutbrod, F. Plasil, R. L. Ferguson, and M. Blann, Phys. Rev. C13, 1483 (1976). M. Beckerman, and M. Blann, BAPS 21, 974 (1976).

16) B. Tamain, F. Plasil, C. Ngô, J. Péter, M. Berlanger and F. Hanappe, Phys. Rev. Lett., 36, 18 (1976).

17) P. R. Christensen and A. Winther, preprint.

FIGURE CAPTIONS

Fig. 1 Integrated laboratory charge distributions for (a) 170 MeV $^{40}Ar + {}^{nat}Ag$ (E/B = 1.2), and (b) 620 MeV $^{86}Kr + {}^{197}Au$ (E/B = 1.4). These distributions have been shifted to align the projectile Z-values and exhibit relatively narrow mass distributions.

Fig. 2 Integrated laboratory charge distributions for (a) 620 MeV $^{86}Kr + {}^{nat}Ag$ (E/B = 1.8) and for (b) 340 MeV $^{40}Ar + {}^{nat}Ag$ (E/B = 2.3). These distributions have been shifted to align the projectile Z-values; they are rather broad and have drifted towards symmetry.

Fig. 3 Center-of-mass angular distributions for (a) 170 MeV $^{40}Ar + {}^{nat}Ag$ (E/B = 1.2), and (b) 620 MeV $^{86}Kr + {}^{197}Au$ (E/B = 1.4). The occurrence of side peaking near the projectile Z is clearly evident (the solid lines drawn through the data points are solely to guide the eye). The number in parenthesis is the common log of the multiplication factor in Fig. 3a whereas in 3b it is the multiplication factor.

Fig. 4 Center-of-mass angular distributions, (a) $(d\sigma/d\theta)$ for 620 MeV $^{86}Kr + {}^{nat}Ag$ (E/B = 1.8) and (b) $(d\sigma/d\Omega)$ for 288 and 340 MeV $^{40}Ar + {}^{nat}Ag$ (E/B = 2.0, 2.3). Here one finds the forward peaking which is typical of lighter ion reactions (the solid lines drawn through the data points are solely to guide the eye). The number in parenthesis in Fig. 4a is the common log of the multiplication factor whereas in 4b it is the multiplication factor.

Table I. Quantities characterizing some heavy ion reactions. All assume an interaction radius $R = 1.07\ (A_1^{1/3} + A_2^{1/3}) + 2.7$ fm [17].

	E_{lab}(MeV)	$E_{c.m.}$(MeV)	B(MeV)	E/B	$\tau(10^{-22}\text{sec})$	$\mu_2\ \frac{(\text{Charge Units})^2}{(10^{-21}\text{sec})}$	$\mu_2\tau$(Charge Units^2)
^{63}Cu + ^{197}Au(a)	365.	277.	250.	*1.11	3.8	6.7	2.6
^{40}Ar + ^{197}Au(b)	220.	183.	163.	*1.12	4.1	6.3	2.6
^{63}Cu + ^{93}Nb(a)	280.	167.	145.	*1.15	4.8	6.2	2.9
^{40}Ar + ^{108}Ag(c)	170.	124.	106.	*1.17	5.0	5.9	3.0
^{63}Cu + ^{197}Au(a)	443.	336.	250.	*1.34	6.9	6.7	4.6
^{136}Xe + ^{197}Au(b)	980.	580.	425.	*1.36	7.7	7.5	5.8
^{86}Kr + ^{197}Au(d)	620.	432.	300.	*1.44	8.2	7.1	5.8
^{136}Xe + ^{159}Tb(b)	980.	528.	361.	*1.46	8.8	7.3	6.4
^{40}Ar + ^{197}Au(e)	288.	239.	163.	*?1.47	8.0	6.3	5.0
^{86}Kr + ^{181}Ta(b)	620.	420.	281.	*1.50	8.8	7.0	6.2
^{86}Kr + ^{159}Tb(b)	620.	402.	255.	1.58	9.6	6.9	**6.6
^{40}Ar + ^{197}Au(e)	340.	283.	163.	1.74	10.0	6.3	**6.3
^{86}Kr + ^{108}Ag(f)	620.	345.	195.	1.78	11.2	6.5	**7.3
^{40}Ar + ^{108}Ag(g)	288.	210.	106.	1.98	12.1	5.9	**7.2
^{40}Ar + ^{108}Ag(g)	340.	248.	106.	2.33	14.2	5.9	**8.4

*Indicates side-peaked angular distributions.
**Indicates that the charge distribution for the relaxed component is broad and exhibits no clear evidence for a peak near the projectile Z.

(a) Ref. 16
(b) Ref. 10
(c) This work
(d) Ref. 9
(e) Ref. 11
(f) Ref. 12
(g) Ref. 6

0 0 0 0 4 7 0 4 9 8 4 6

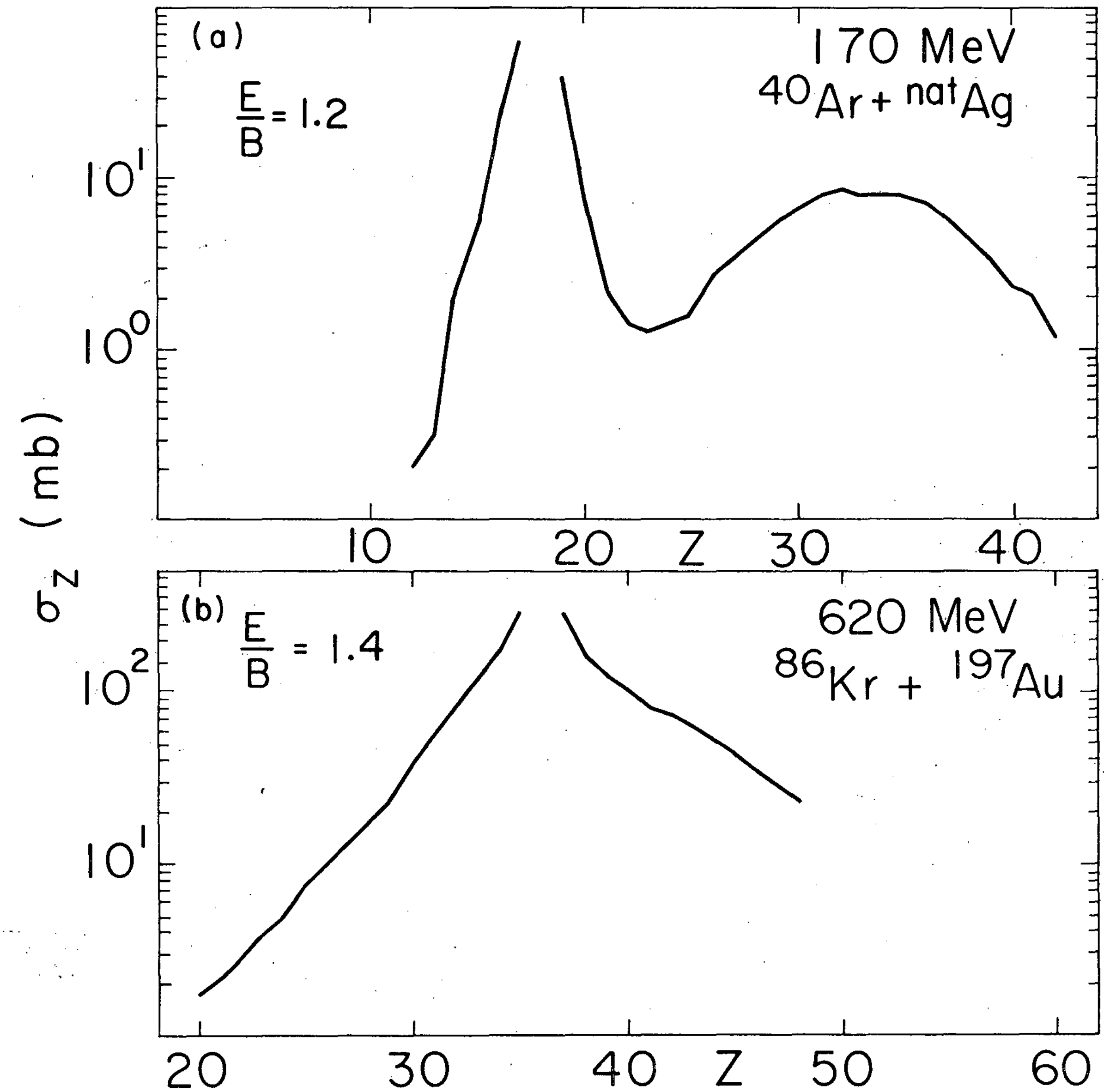

XBL7612-11057

Fig. 1

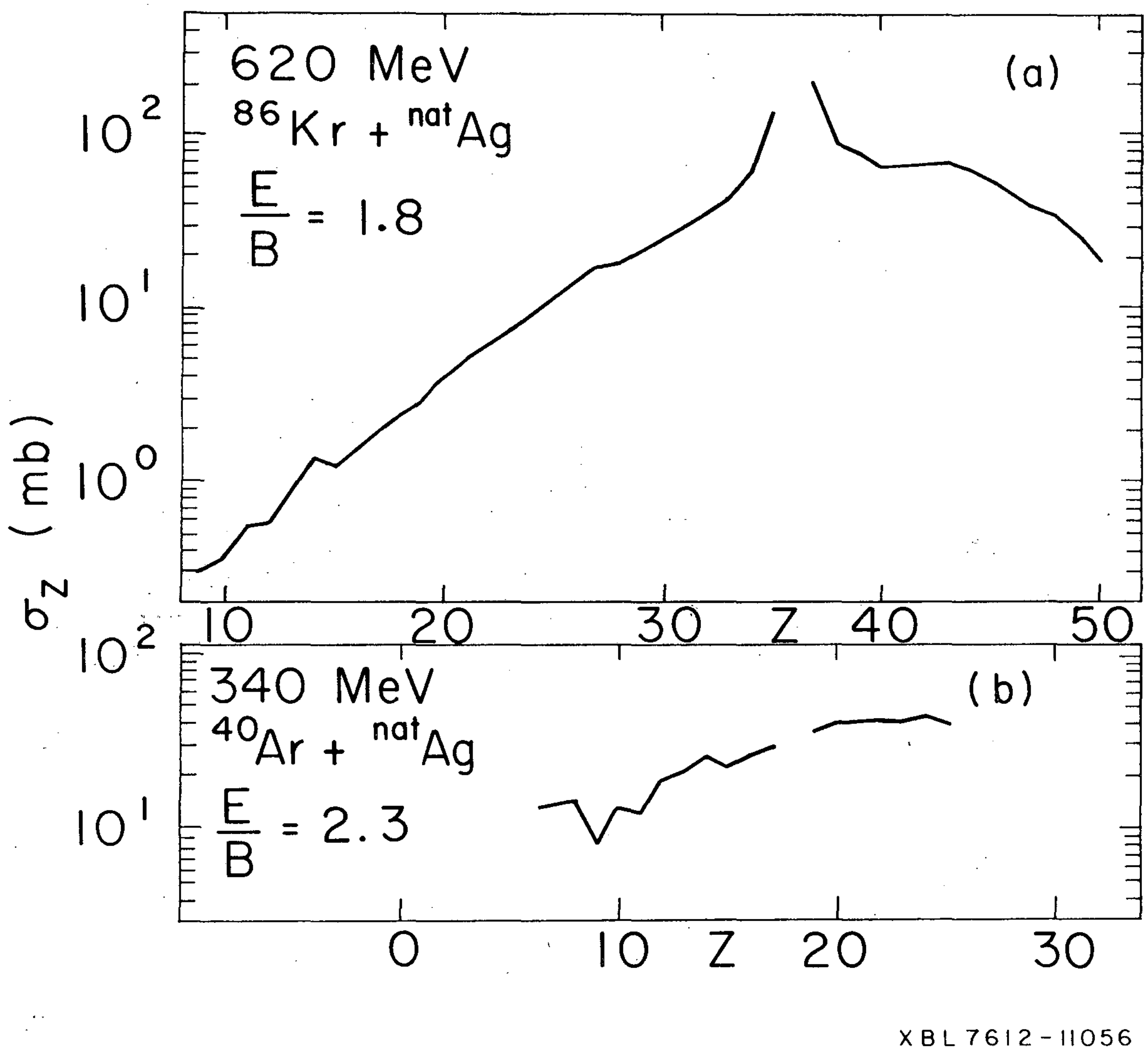
620 MeV
^{86}Kr + ^{nat}Ag
$\frac{E}{B}$ = 1.8
(a)
σ_Z (mb)
10^2
10^1
10^0
10
20
30
Z
40
50
340 MeV
^{40}Ar + ^{nat}Ag
$\frac{E}{B}$ = 2.3
(b)
10^2
10^1
0
10
Z
20
30
XBL 7612-11056

Fig. 2

0 0 0 0 4 7 0 9 8 5 7

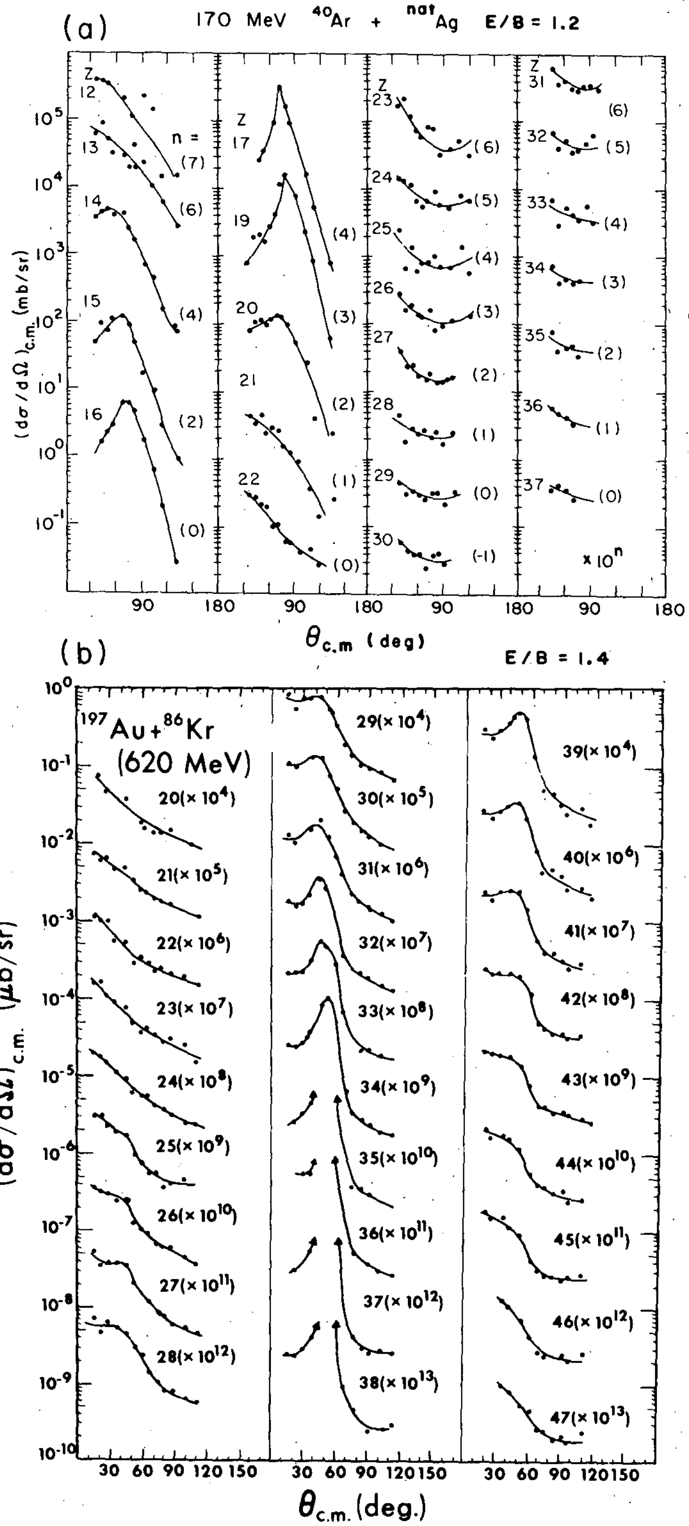

XBL 7612-10982

Fig. 3

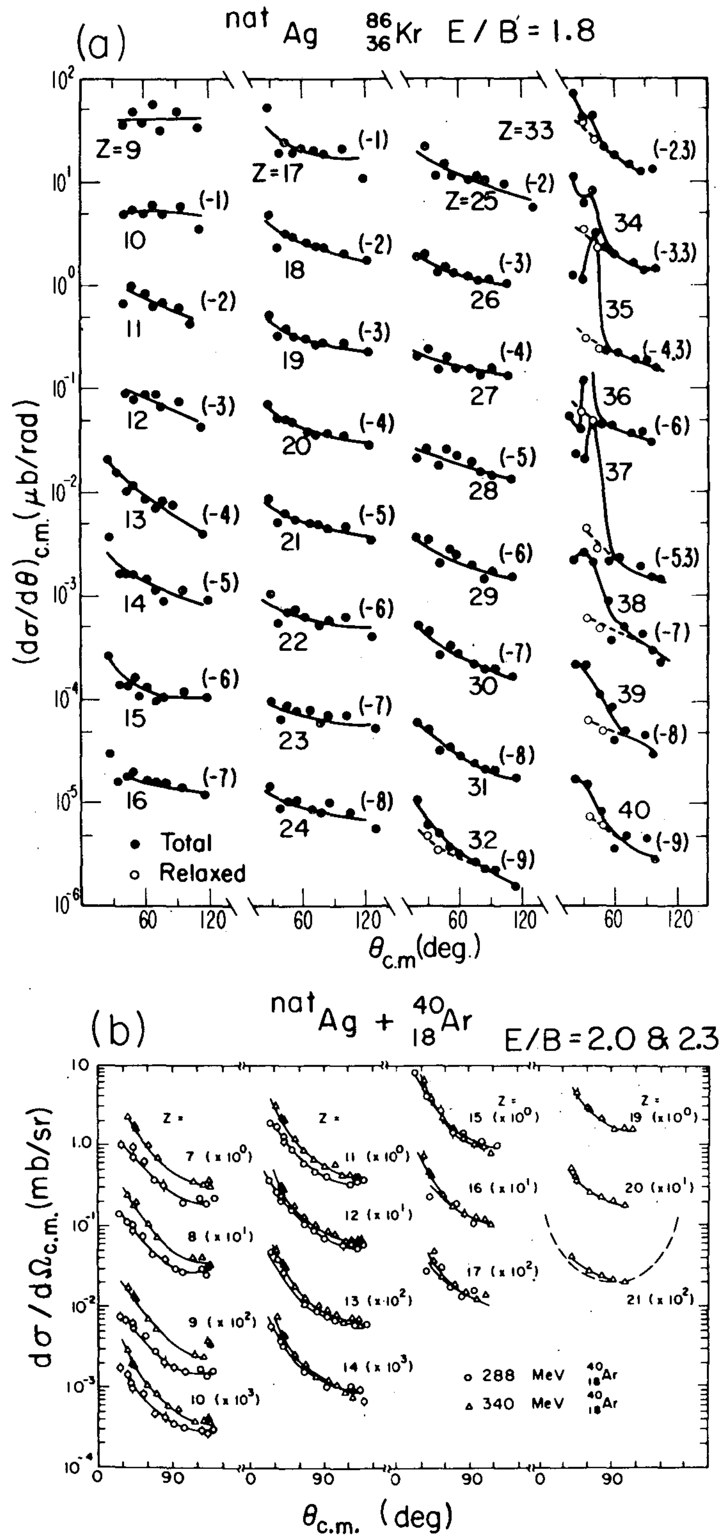

XBL 7612-10981

Fig. 4

TECHNICAL INFORMATION DIVISION
LAWRENCE BERKELEY LABORATORY
UNIVERSITY OF CALIFORNIA
BERKELEY, CALIFORNIA 94720